

Supplemental Information

Rankin et al Figure S1 relevant to Figure 1.

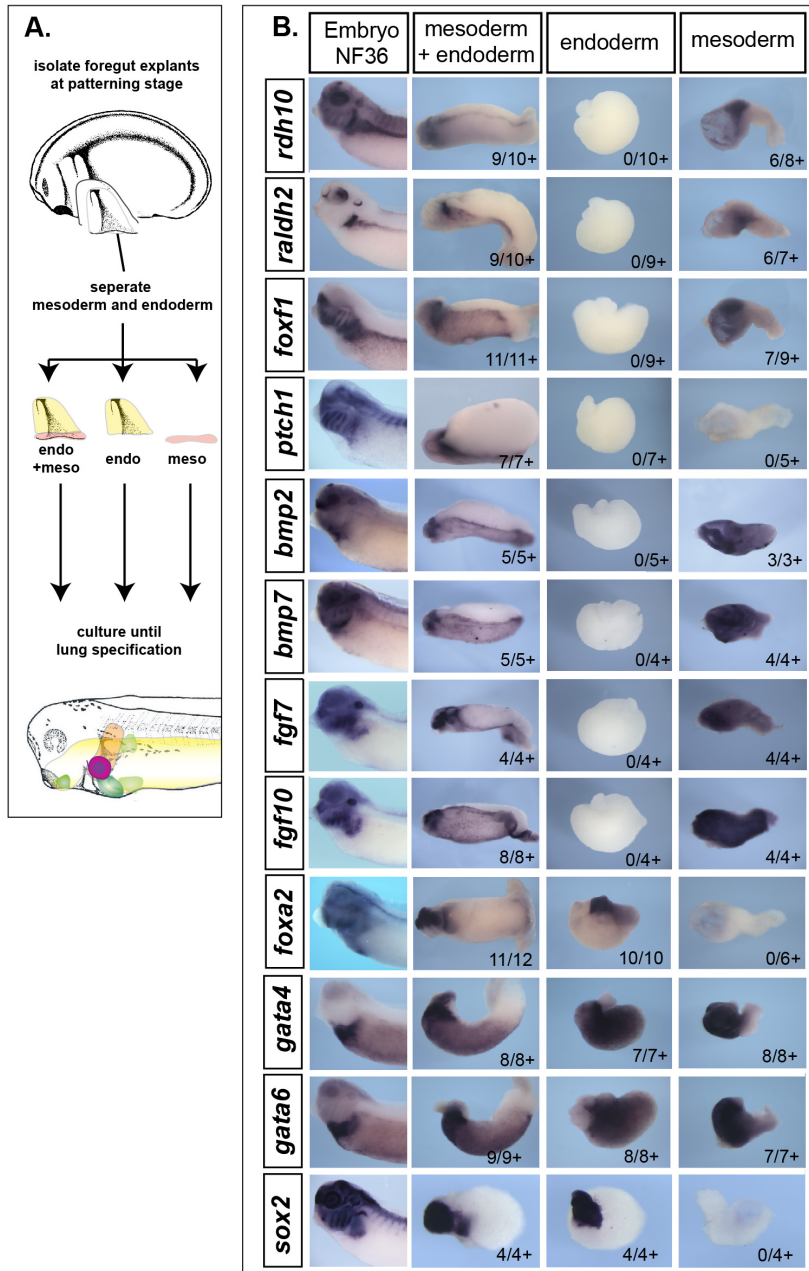


Figure S1 relevant to Figure 1. Additional analysis of gene expression in *Xenopus* foregut explants.

(A) Schematic of the *Xenopus* specification assay culturing foregut endoderm (yellow) and mesoderm (orange) together or separately from NF20 to NF36.

(B) In situ hybridization of stage NF36 embryos and explants using the indicated probes. The number of explants robustly expression the gene is indicated in the lower right of each panel.

Rankin et al Figure S2 relevant to Figure 2.

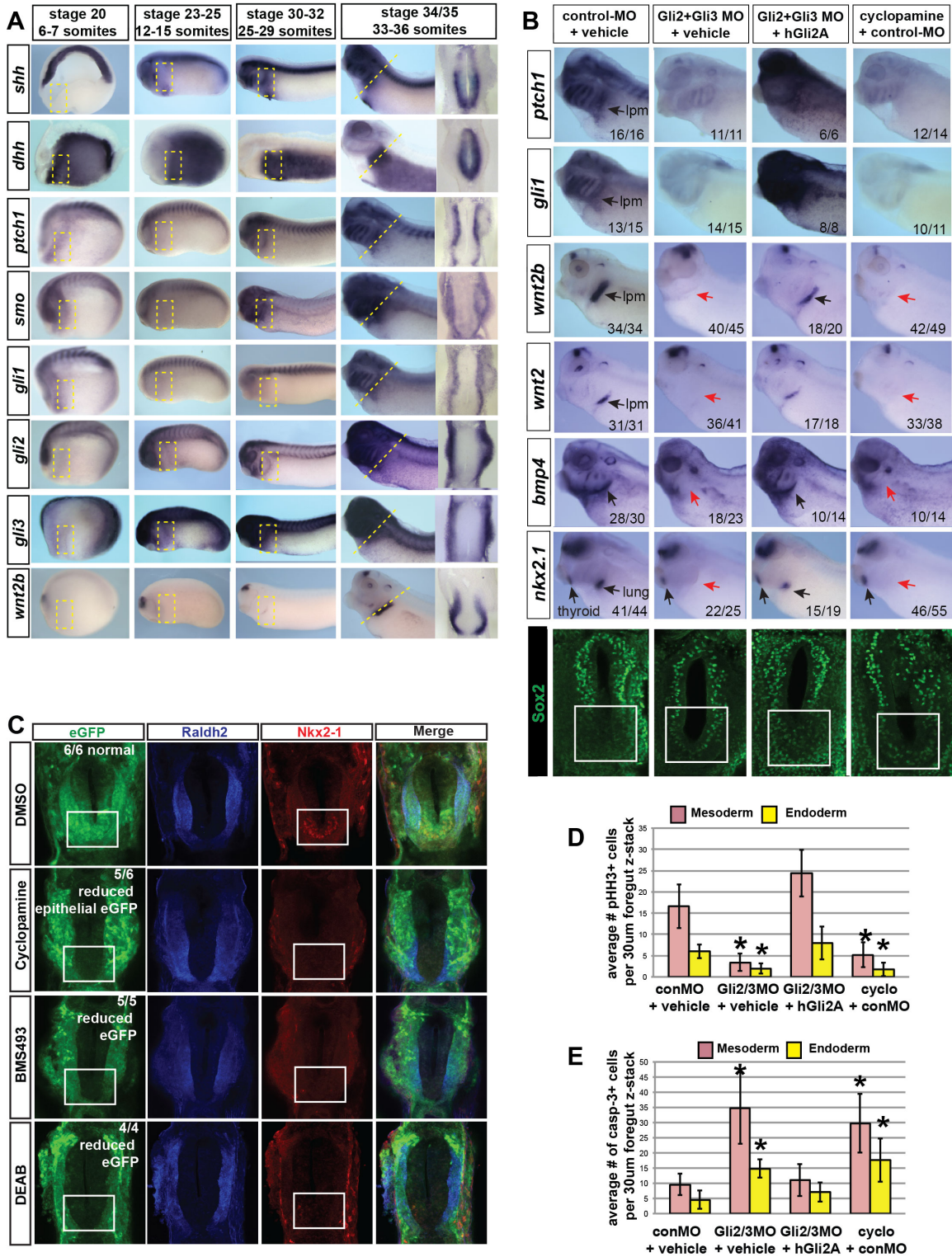


Figure S2 relevant to Figure 2. Additional analyses of the Hh/Gli pathway function in *Xenopus*.

(A) In situ hybridization of Hh pathway components during different stages of *Xenopus* development prior to and during lung induction. The foregut / presumptive lung region (boxed) and sections through the lung field (dashed line) are shown at NF34/35. Robust expression of the HH target genes *ptch1* and *gli1* in the foregut region is not detectable until NF30-32, coincident with the timing of *shh* induction in the foregut region. *Smo*, *gli2*, and *gli3* are expressed in foregut mesoderm but not endoderm. *Wnt2b* is robustly detected at NF34/35 but not at earlier stages

(B) In-situ hybridization using the indicated probes on NF34 embryos that were either injected at the 4/8-cell stage into the presumptive foregut mesendoderm with control-MO (20 ng), Gli2+Gli3-MOs (10 ng each), or treated with vehicle or Cyclopamine from NF20-34. Red arrows indicate regions of reduced or absent gene expression in the foregut domain. Loss / severe reduction of *ptch1* and *gli1* confirms the effective reduction in Hh signaling activity, and co-injection of an RNA encoding an hGli2A (125 pg) rescued lung development confirming the specificity of the Gli2/3-MO depletion. Sox2 immunofluorescence (green) shows abnormal expression of Sox2 in the ventral foregut (boxed area) of cyclopamine-treated and Gli2/3-MO-injected embryos. Abbreviations: lpm; lateral plate mesoderm. The number of embryos exhibiting the phenotype is indicated in the lower right of each panel.

(C) Pharmacological disruption of the Hh and RA pathways results in a loss of Wnt/bcatenin reporter activity in the ventral foregut endoderm. Transgenic *X. tropicalis* *Tg(7xtcf:eGFP)* embryos were treated with cyclopamine from NF20-34 or with BMS493 (pan-RAR antagonist) or DEAB (aldehyde dehydrogenase inhibitor) from NF15 to 25. Wnt-reporter activity was assayed at NF34 by GFP immunofluorescence (green). Sections were co-stained with Raldh2 (blue) and Nkx2-1 (red) antibodies, indicating the lpm and respiratory epithelium respectively. White boxed area indicates the ventral foregut.

(D) Quantification of mitotic cell number by phospho-Histone H3 (pHH3) staining in control and HH pathway-disrupted embryos at NF35. The average number of pHH3+ cells observed in either the endoderm (yellow bars), or mesoderm (pink bars) were quantified from 30 μ M confocal z-stacks of the foregut (n=5 embryos per condition). Error bars +/- standard deviation; * p<0.05 in student t-test relative to controls. Abbreviations: cyclo, cyclopamine.

(E) Quantification of apoptosis by activated caspase-3 (casp-3) immunofluorescence in control and HH pathway-disrupted embryos at NF41. The average number of casp-3+ cells in either the endoderm (yellow bars) or mesoderm (pink bars) were quantified from 30 μ M confocal z-stacks of the foregut (n=5 embryos per condition). Error bars +/- standard deviation; * p<0.05 in student t-test relative to controls. Abbreviations: cyclo, cyclopamine.

Rankin et al Figure S3 relevant to Figure 3.

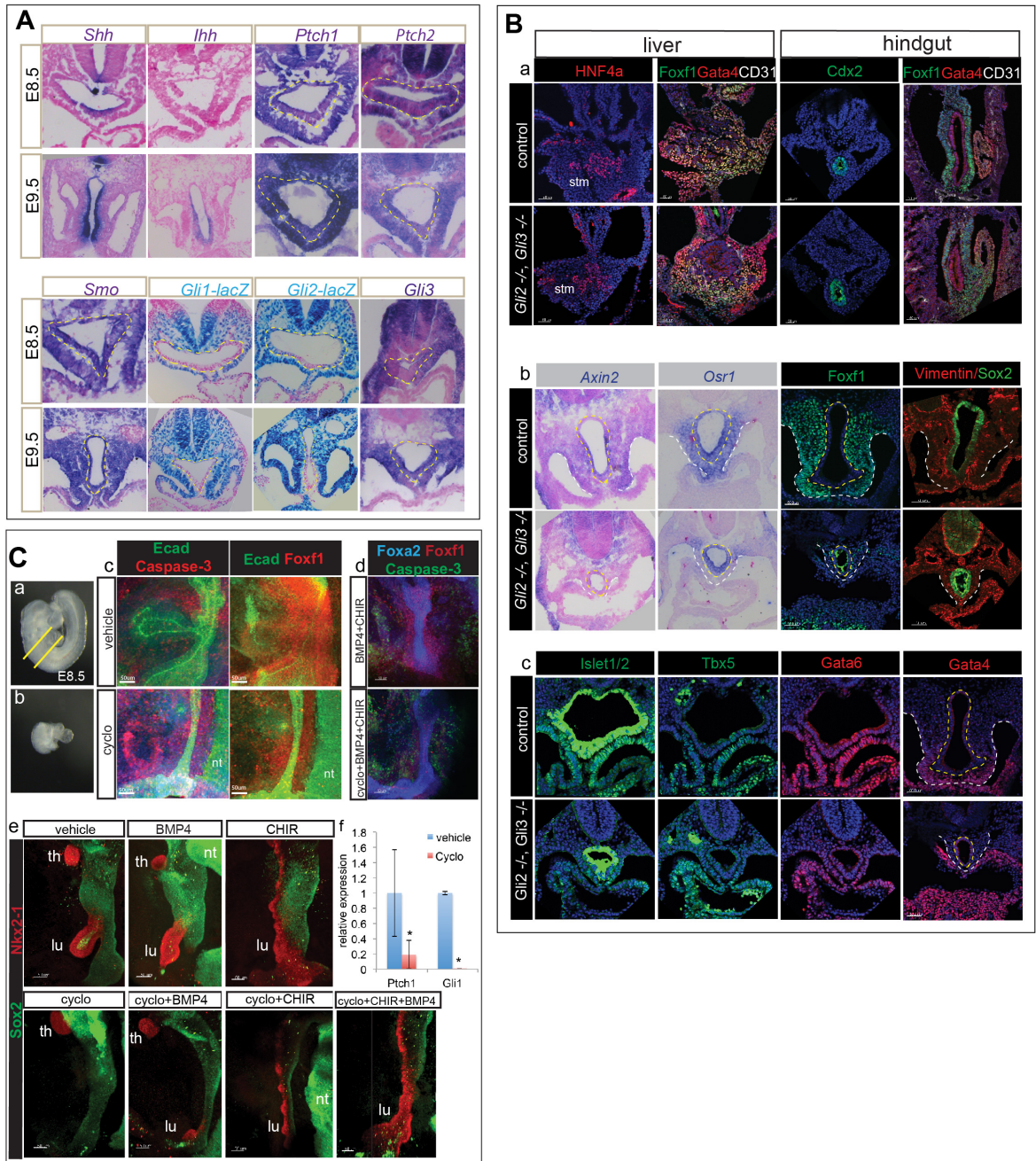


Figure S3 relevant to Figure 3. Additional analyses of the Hh/Gli pathway and HhGli loss-of-function during mouse development

(A) Expression of Hh pathway components in the E8.5 and E9.5 mouse foregut. Yellow dashed line outlines the endoderm. In-situ hybridization or bgal staining sections from transgenic embryos show that *Shh* and *Ihh* ligands are expressed in the endoderm, *Ptch1*, *Ptch2* and *Smo* are expressed in both the mesoderm and endoderm, whereas *Gli1-lacZ*, *Gli2-lacZ* and *Gli3* transcripts are predominantly expressed in the splanchnic lpm.

(B) Analysis of additional epithelial and mesenchymal markers in E9.5 (23-28s) control and *Gli2^{-/-};Gli3^{-/-}* embryos. (a) Immunostaining of hepatoblasts (HNF4a), visceral mesenchyme (Foxf1 and Gata4), endothelial cells (CD31), and hindgut epithelium (Cdx2) indicate that the liver bud and intestine are not obviously different between control and mutant. (b-c) In-situ hybridization of the Wnt-target gene *Axin2* shows that Wnt/b-catenin signaling is compromised in the hypoplastic foregut of *Gli2/3* mutants. In situ and immunostaining of transcription factors *Osr1*, Foxf1, Gata4, Gata6, Islet1/2, Txb5 indicate cardio-pulmonary mesenchyme development is compromised in the hypoplastic lpm of *Gli2/3* mutants. Vimentin positive mesenchyme is still present around the hypoplastic Sox2⁺ foregut of *Gli2/3* mutants. Yellow dashed line outlines the endoderm and white dashed line outlines the foregut mesoderm.

(C) Mouse foregut explant culture assays. Brightfield images of an E8.75 mouse embryo (a) showing the dissected foregut region (b). (c-e) Wholemount immunostaining of explants after 2 days of culture in either vehicle or the indicated combination of inhibitor/agonist. Cyclopamine (cyclo) treatment results in failed induction of Nkx2-1+ lung epithelium and elevated cell death the epithelium and mesenchyme; co-treatment of cyclopamine with CHIR+BMP4 robustly rescues Nkx2-1+ respiratory fate. Abbreviations, lu, lung; nt, neural tube; th, thyroid. (f) qRT-PCR analysis of DMSO or cyclopamine-treated foregut explants for the Hh/Gli target genes *Ptch1* and *Gli1* demonstrates effective Hh inhibition. Error bars +/- standard deviation. *p<0.05 is pairwise student T-test relative to no RA control.

Rankin et al Figure S4A-D relevant to Figure 4.

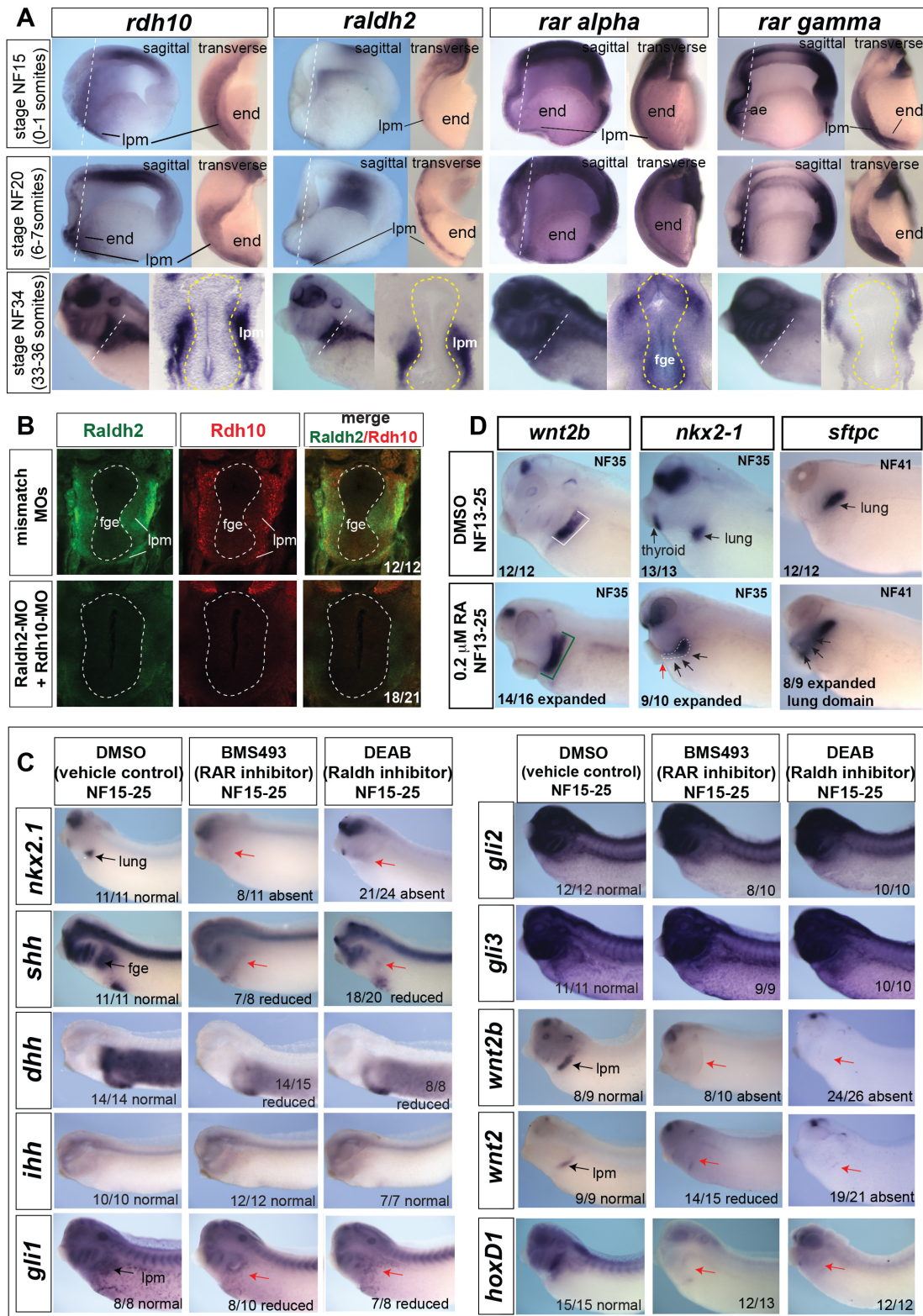


Figure S4A-D relevant to Figure 4. Additional analyses of RA loss-of-function in *Xenopus*

(A) In situ hybridization of RA pathway components at stages NF15, NF20, and NF34. For stages NF15 and 20 sagittal and transverse views of bisected embryos are shown. Dashed white line on the sagittal view shows plane of section shown in the transverse view. For NF34, white dashed line indicates plane of section shown; yellow dashed line outlines the endoderm. Expression of *raldh2* is restricted to the mesoderm at all stages examined, whereas *rar alpha* is detected in both mesoderm and endoderm at all stages examined. *Rar gamma* is expressed in the anterior-most endoderm and mesoderm at NF15 and NF20, however is down-regulated in the foregut by NF34. Abbreviations: lpm, lateral plate mesoderm; end, endoderm; ae, anterior endoderm; fge, foregut endoderm.

(B) Immunofluorescence of the NF34 *Xenopus* foregut region from control and *rdh10*-MOs + *raldh2*-MO-injected embryos confirms effective *Rdh10* and *Raldh2* knockdown in the foregut lpm. Abbreviations: fge, foregut endoderm; lpm, lateral plate mesoderm. Numbers in the lower right corner indicate the numbers of embryos with the observed staining pattern.

(C) Treatment of *Xenopus* embryos from NF15-25 with 10 μ M BMS493 (pan RAR-antagonist) or 20 μ M DEAB (aldehyde dehydrogenase inhibitor) phenocopies the *Rdh10*+*Raldh2* MO knockdown phenotype. In situ hybridization at NF34 using the indicated probes. Red arrows indicate regions of severely reduced or absent gene expression in the foregut domain. Abbreviations: fge, foregut endoderm; lpm, lateral plate mesoderm. Numbers in the lower right corner indicate the numbers of embryos with the observed staining pattern.

(D) RA gain-of-function results in an expansion of the respiratory field. *Xenopus* embryos were treated from NF13-25 with either DMSO vehicle or 0.2 μ M of RA, cultured until either NF35 or NF41, and then assayed by in situ hybridization for expression of the indicated genes. Exogenous RA expands the *nkx2-1*+ and *sftpc*+ respiratory field throughout the pharyngeal region (black arrows), and inhibits thyroid expression of *nkx2-1* (red arrow)

Rankin et al Figure S4E relevant to Figure 4.

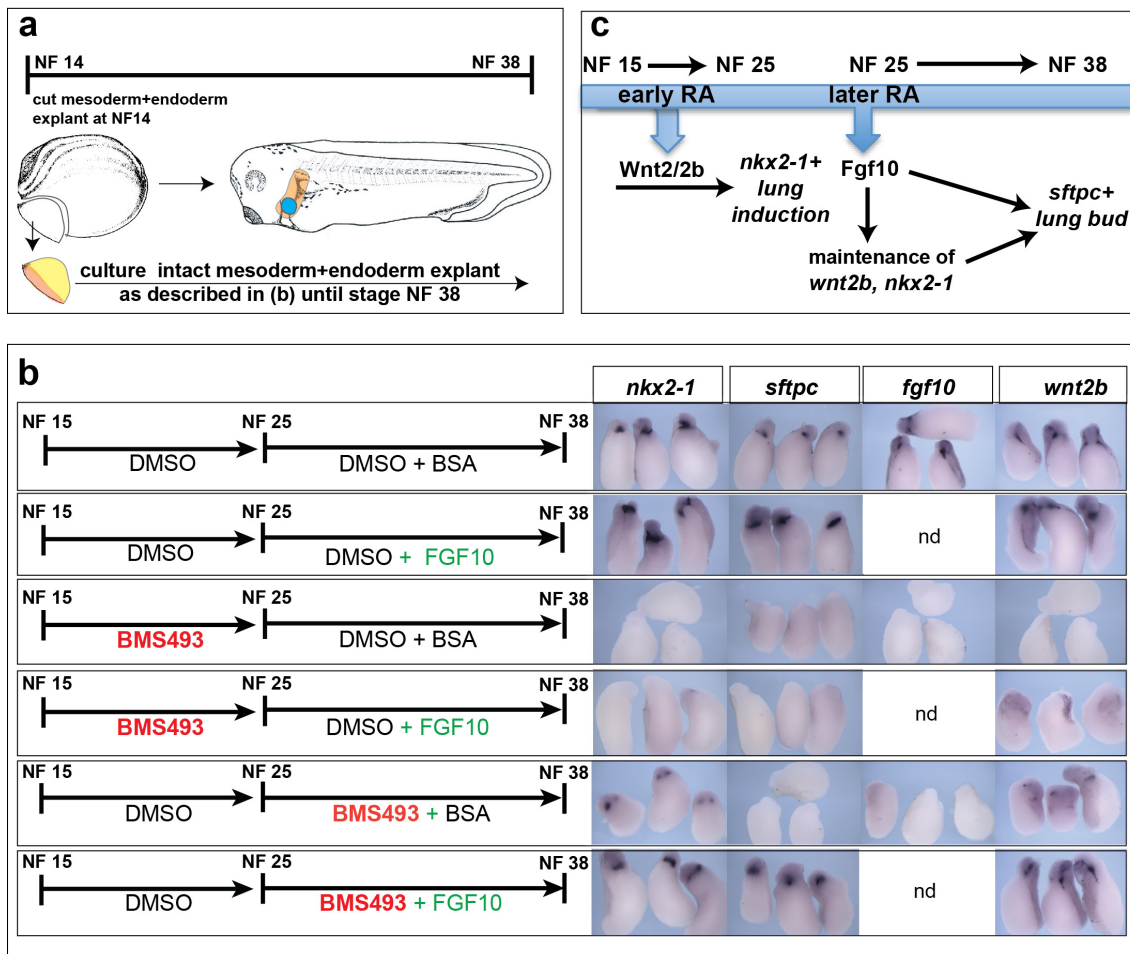
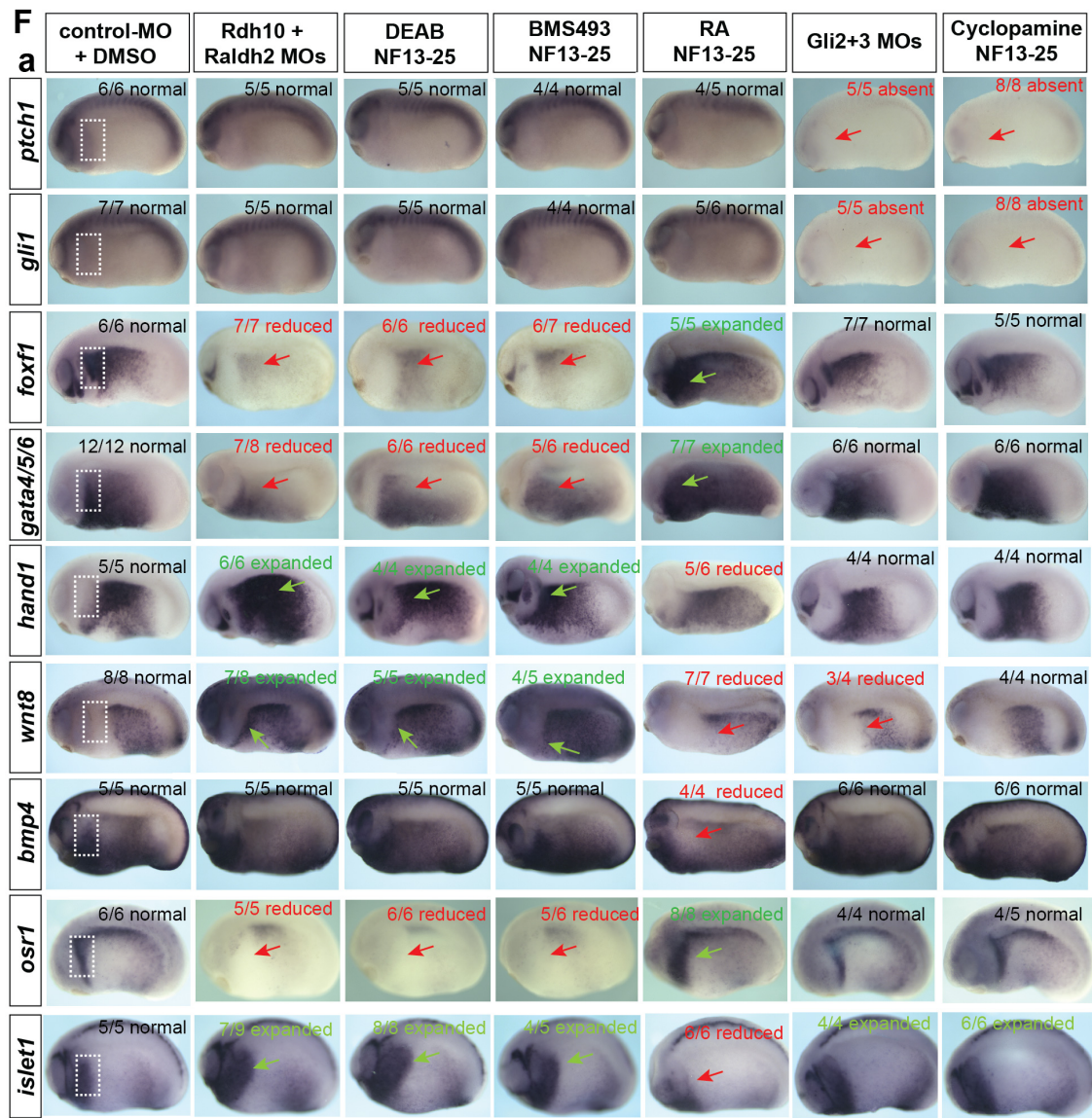


Figure S4E relevant to Figure 4. RA has temporally distinct functions in *Xenopus* lung development.

(a,b) A schematic of the experimental design. Intact foregut explants (endoderm + mesoderm) were dissected at NF14 and cultured as describe in (b) until NF38. In-situ hybridization of foregut explants at NF38 shows that BMS493 treatment from NF15-25inhibits expression of *nkx2-1* and *wnt2b*; expression of these genes cannot be rescued by culture with exogenous FGF10. In contrast BMS493 treatment from NF25-35 reduces expression of *nkx2-1*, *wnt2b* and inhibits expression of *sftpc*; however exogenous FGF10 is able to rescue expression of these genes when added during the NF25-38 time period. The two temporal roles for RA signaling are diagrammed in (c).

Rankin et al. Figure S4F relevant to Figure 4.



b Model of lpm patterning

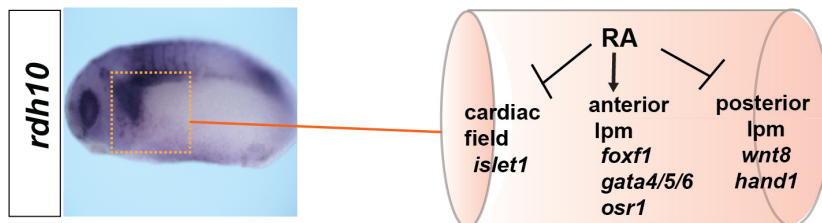


Figure S4F relevant to Figure 4. RA regulates early lpm patterning.

(F) RA regulates early lpm patterning independent of Hh. (a) Embryos were injected at the 4-8 cell stage in the dorsal marginal zone with the indicated MOs or treated from stages NF13-25 with either DEAB (10 μ M), BMS493 (10 μ M), RA (0.2 μ M), or Cyclopamine (80 μ M). In-situ hybridization with the indicated probes was performed at NF25. Red arrows indicate reduced expression and green arrows expanded expression. The boxed white region indicates a domain of anterior lateral plate mesoderm that robustly expresses *foxf1*, *gata4/5/6*, and *osr1*. *islet1* is a marker of the heart field. The mid/hindgut lateral plate mesoderm markers *hand1* and *wnt8* are excluded from this boxed anterior lpm domain in control embryos. RA pathway disruption (via *Rdh10*+*Raldh2*-MO injection, DEAB, or BMS493-treatment), but not HH pathway disruption (via *Gli2*+3-MO injection or cyclopamine treatment), results in a severe reduction of the anterior lpm domain of *foxf1*, *gata4/5/6*, and *osr1* and an anterior expansion of the *wnt8* and *hand1* domains. Exogenous RA treatment has the opposite effect and expands the *foxf1*, *gata4/5/6*, and *osr1* domains and down-regulates/reduces the *wnt8* and *hand1* domains. (b) *rdh10* expression at stage NF25 with a model illustrating how early RA patterns the lpm by promoting the formation of an anterior foregut lpm domain characterized by expression of *foxf1*, *gata4/5/6*, and *osr1* and suppressing the posterior mid/hingut fate as characterized by *wnt8* and *hand1*.

Rankin et al Figure S5 relevant to Figure 5.

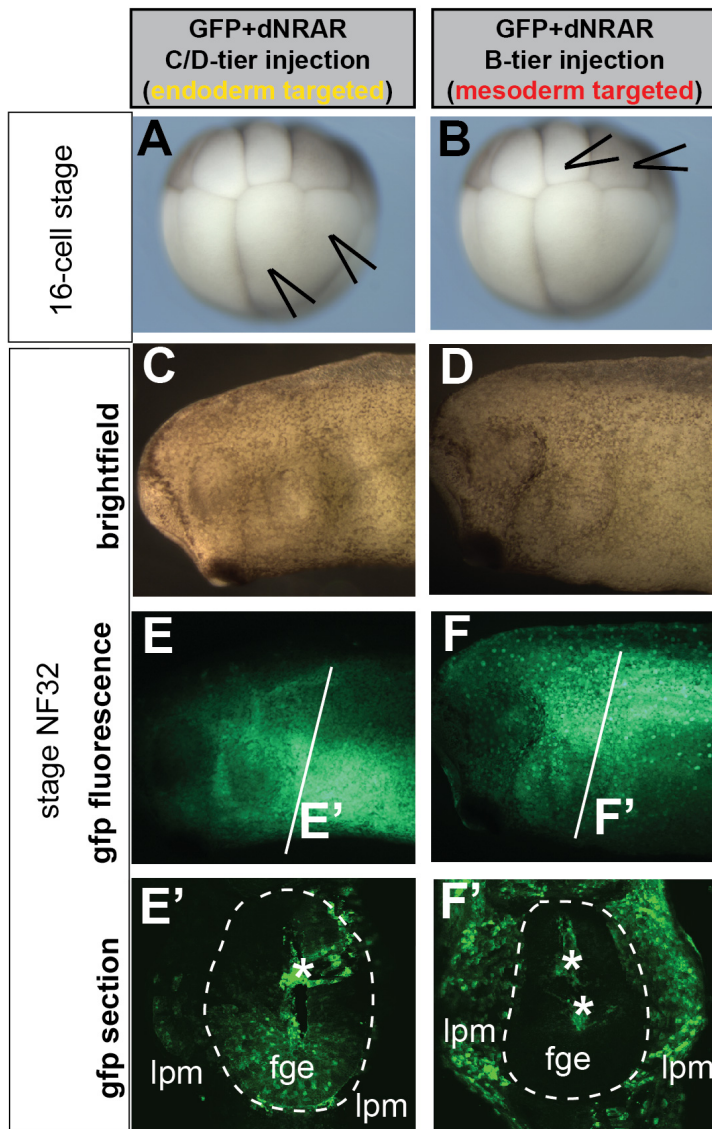


Figure S5 relevant to Figure 5. Lineage tracing of targeted injections into the *Xenopus* foregut mesoderm or foregut endoderm.

(A,B) Brightfield images of *Xenopus* embryos at the 16-cell stage. Black arrows indicate the blastomeres injected to target either endoderm (A) or mesoderm (B).

(C,D) Brightfield and (E,F) fluorescence images of NF32 embryos showing localization of the descendants of the injected blastomeres. White lines in E, F indicate plane of section (sections shown in E', F'). White asterisks indicate some cells sloughed off into the endodermal lumen (a common event) and white dashed line signifies the endoderm-mesoderm boundary. Abbreviations: fge, foregut endoderm; lpm, lateral plate mesoderm

Supplemental Experimental Procedures

Xenopus Methods

For *Xenopus* injection experiments, morpholino oligos (MOs) were purchased from Gene Tools LLC and mRNAs were synthesized using the Ambion mMessage mMachine SP6 or Megascript T7 kits according to manufacturer's instructions. 15 ng of previously validated MOs targeting Gli2, Gli3, Raldh2, and Rdh10 (Nguyen et al., 2005; Strate et al., 2009) or mRNA encoding hGli2A (125 pg; Roessler et al., 2005) or dnRAR (Sharpe and Goldstone, 1997) were injected at the 4-cell stage into the dorsal marginal zone (DMZ) of both dorsal blastomeres (7.5 ng in a volume of 4 nL per blastomere) to target the foregut mesendoderm. For hGli2A rescue experiments, hGli2A mRNA (62.5 pg in a volume of 4 nL per blastomere) was subsequently injected at the 8-cell stage into the similar DMZ region. For targeted injection of the dnRAR mRNA in Figure 5 (200 pg in a volume of 4 nL per blastomere), embryos at the 16/32-cell stage were injected in either B-tier or C/D-blastomeres as shown in supplemental figure S5 to target either the mesoderm or endoderm respectively.

Whole *Xenopus* embryos were treated with the following small molecule concentrations: 80 mM cyclopamine (Tocris Bioscience 1623); 10 μ M BMS493 (Tocris Bioscience 3509), 20 μ M DEAB (Sigma D86256), 20 μ M SAG (Tocris Bioscience 4366), 8 μ M BIO (Tocris Bioscience 3194), and 0.2 μ M all-trans RA (Sigma R2625). Equal concentrations of vehicle (DMSO or ethanol) were used on sibling embryos. All microinjection or inhibitor treatment experiments were repeated a minimum of three times, all with similar effects on the markers analyzed. For *Xenopus* in-situ hybridization analyses, DIG-labeled antisense RNA probes were generated using linearized full-length cDNA plasmid templates; plasmid details are available upon request and were either purchased from GE Dharmacon or provided by the *Xenopus* community. Complete details describing probe synthesis and the in-situ hybridization protocol are available on Xenbase (<http://wiki.xenbase.org/xenwiki/index.php/Protocols>). Immunostaining on bisected *Xenopus* foregut regions was performed as described (Rankin et al. 2012) using the antibodies listed in supplemental table S1. For quantification of the number of active-caspase 3 and phosph-histone H3 positive nuclei in the *Xenopus* foregut endoderm or mesoderm, the anti-Fibronectin 4H2 antibody was used as a counterstain, which enables the 2 layers to be discerned. The average number of positive nuclei were counted using Image-J software from 30 μ M optical z-stacks through the bisected foregut regions of n=5 embryos per condition. Pairwise student T-tests between control and experimental were used to determine statistical significance *p<0.05.

For *Xenopus* explant studies, foregut tissue was micro-dissected in 1XMBS +4%Ficoll+ 50 mg/mL gentamycin. To separate the endoderm from the mesoderm/ectoderm, explants were then incubated for 10 minutes in 0.5X MBS+ 5 U/mL Dispase (Fisher Scientific CB-40235) and then the germ layers were manually separated with an eyebrow knife and forceps. Isolated endoderm, mesoderm/ectoderm, or intact explants were cultured in 0.5X MBS + 0.1% BSA + 50 mg/mL gentamycin with the following concentrations of small molecules or recombinant proteins: 200 ng/mL Fgf10; 50 ng/mL Bmp4 (both from R&D Systems); 5 μ M Bio, 0.2 μ M RA, 1 μ M BMS493. Equal concentrations of vehicle (DMSO and/or PBS+0.1%BSA) were used as controls.

Mouse methods

Mouse embryos were harvested at indicated developmental stages and fixed in 4% paraformaldehyde in PBS at 4°C overnight and then washed in PBS. For mouse whole-mount immunostaining, embryos were serially dehydrated into 100% methanol and stored at -20°C. Embryos were then brought to room temperature and incubated in Dent's bleach (80% methanol / 10% DMSO / 10% 37% hydrogen peroxide) for 2 hours at room temperature. After serial rehydration into PBS, embryos were blocked in 5% normal donkey serum (Jackson ImmunoResearch) in PBSt (PBS +0.5% triton) for 2 hours at room temperature and then incubated in primary antibodies (listed in supplemental table S2) diluted in block overnight at 4°C. After five 1-hour washes with PBSt, embryos were incubated in secondary antibody overnight at 4°C (Jackson ImmunoResearch; all raised in donkey) diluted 1:500 in PBSt. After an additional five to seven PBSt washes, embryos were dehydrated directly into 100% methanol and cleared in Murray's clear (2 parts

benzyl benzoate / 1 part benzyl alcohol) prior to confocal imaging on a Nikon A1Rsi inverted confocal microscope.

For immunostaining on frozen sections, fixed embryos were washed in PBS, embedded in OCT, and cryo-sectioned at 10 μ m thickness. Sections were blocked as described for whole-mount and then incubated in primary antibody (listed in supplemental table S2) overnight at 4^oC. After five 1-hour PBSt washes, sections were incubated in secondary antibodies at room temperature for 1.5 hours. Confocal images were captured on a Nikon A1Rsi inverted confocal microscope. To quantify the numbers of phospho-histone H3+ (pHH3) and activated Caspase 3+ (Casp3) cells on mouse foregut frozen sections (n=3 foregut sections from n=3 control or Gli2/3 mutant embryos at each stage), nuclei were counterstained endoderm cells (E-cad+/FoxA2+) from mesoderm cells (E-cad-/FoxA2-). The total numbers of foregut cells per section were counted based on the nuclear DAPI signal using IMARIS software and then the average % pHH3 or Casp3 positive cells was calculated. Pairwise student T-tests between control and mutants were used to determine statistical significance *p<0.05.

For mouse in-situ hybridization, DIG-labeled probes were generated using linearized full-length mouse *Osr1*, *BMP4*, *Shh*, *Ihh*, *Gli1* cDNA plasmids kindly provided by Dr. Rulang Jiang; full-length *Wnt2*, *Wnt2b*, *Ptch1*, *Ptch2*, *Smo*, and *Gli3* cDNA plasmids were purchased from GE Dharmacon.

For E8.5 mouse explants the foregut was dissected and cultured on air-liquid interface in BGJb medium (Thermo Scientific 12591-038) with 10% fetal bovine serum, 1 mg/ml l-ascorbic acid and antibiotics. For whole mouse embryo cultures, E7.5 embryos were cultured on a roller culture apparatus (BTC Engineering, Cambridge, UK) in a 1:1 mixture of Ham's F12 medium and whole embryo culture rat serum (Harlan Labs) containing N-2 Supplement (Invitrogen). Both the E7.5 and E8.5 cultures were maintained for 2 days at 37oC and gassed with 20% O₂, 5% CO₂ supplemented with either 6 μ M Cyclopamine (Tocris Biosciences), 1 μ M Chiron (Tocris Biosciences), and/or 20 ng/mL recombinant hBMP4 (R&D Systems), and 10 μ M BMS493 (Tocris Biosciences).

Human ES cell RNA isolation, qPCR, and immunostaining methods

Total RNA was isolated from hESc cultures using the Nucleospin RNA II kit (Machery-Nagel). Reverse transcription was performed from 100 ng RNA using Superscript VILO cDNA Synthesis Kit (Invitrogen) according to manufacturer's protocol. qPCR was performed using Quantitect SybrGreen Master Mix (Qiagen) on a CFX-96 Real-time PCR Detection System (BioRad). Gene expression analysis was determined using the Δ CT method. PCR primers and are listed in supplemental table S3. Immunostaining of the monolayer cultures was performed as described in McCracken et al. 2014 using the antibodies listed in supplemental table S2.

Table S1. Antibodies used in Mouse Immunofluorescence.

Antibody	Company /Cat#	Made in	Dilution
Active caspase-3	BD Pharmingen / 559565	rabbit	1:500
CD31	BD Pharmingen / 550274	rabbit	1:400
Cdx2	BioGenex / MU392A-UC	mouse	1:500
E-cadherin	R&D Systems / MAB7481	rat	1:1000
FoxA2	Santa Cruz / sc-6554	goat	1:500
Foxf1	R&D Systems / AF4798	goat	1:500
Gata4	Santa Cruz / sc-1237	goat	1:400
Gata6	R&D Systems / AF1700	goat	1:500
phospho-Histone H3	Cell Signaling / 9701L	rabbit	1:500
Islet1/2	Dev.Studies HB / 39.4D5-c	mouse	1:100
Nkx2-1	Santa Cruz / sc-13040X	rabbit	1:500
phospho-Smad1/5/8	Millipore / AB3848	rabbit	1:500
Sox2	Abcam / ab79351	mouse	1:500
Tbx5	R&D Systems / AF5918	sheep	1:500
Vimentin	Santa Cruz / sc-7557	goat	1:500

Table S2. Antibodies used in *Xenopus* Immunofluorescence

Antibody	Company / Cat#	Made In	Dilution
active caspase-3	BD pharmingen / 559565	rabbit	1:1000
Acetylated Tubulin	Sigma / T7451	mouse	1:1000
eGFP	Clontech/ 632569	mouse	1:500
Fibronectin 4H2	DeSimone Lab	mouse	1:1000
Foxf1	R&D systems / AF4798	goat	1:500
phospho-Histone H3 (Ser10)	Cell Signaling / 9701	rabbit	1:500
Nkx2.1	Santa Cruz / sc-13040X	rabbit	1:300
phospho-Smad1/5/8(9)	Cell Signaling / 138D20	rabbit	1:500
Raldh2	Santa Cruz / sc-22591	goat	1:500
Rdh10	Antibody Verify / AAS17532C	rabbit	1:300
Sox2	Abcam / 79351	mouse	1:1000

Table S3. qPCR primer sequences for human gene expression analysis in Figure 7.

Target	Forward Primer	Reverse Primer
<i>FOXA1</i>	GCCTGAGTTCATGTTGCTGA	CTGTGAAGATGGAAGGGCAT
<i>GAPDH</i>	CCCATCACCATCTTCCAGGAG	CTTCTCCATGGTGGTGAAGACG
<i>NKX2.1</i>	CTCATGTTTCATGCCGCTC	GACACCATGAGGAACAGCG
<i>SOX2</i>	GCTTAGCCTCGTCGATGAAC	AACCCCAAGATGCACAACCTC

